ChemCatChem

Research Article
doi.org/10.1002/cctc.202401002

Chemistry Europe
European Chemical Societies Publishing

www.chemcatchem.org

# Plasmonic Membrane for $TiO_2$ Nanoparticles Activity Detection in Complex Environments

Ecem Tiryaki,[a, b] Ana Sousa-Castillo,*[a, b] Laura Rodríguez-Lorenzo,[c] Begoña Espiña,[c] Ramón A. Alvarez Puebla,*[d, e] and Miguel A. Correa-Duarte*[a, b]

Titanium dioxide nanoparticles ($TiO_2$NPs) are widely manufactured semiconductors, but their release into aquatic environments poses significant threats to ecosystems and human health. The environmental hazard associated with $TiO_2$NPs in surface water primarily results from their photocatalytic activity, which generates reactive oxygen species (ROS). Addressing this challenge is crucial for ensuring the safe utilization of $TiO_2$NPs and preserving the environment. In this study, we developed a novel plasmonic membrane comprising titanate nanowires (TiNWs) functionalized with silica-coated gold nanostars (AuNSts) to probe, in situ, the capture and measurement of the photocatalytic activity of $TiO_2$NPs in complex media such as seawater. This method represents a unique and precise approach to real-time monitoring of the presence and photocatalytic activity of $TiO_2$NPs, thereby laying the foundation for establishing an environmental risk parameter for these particles.

## 1. Introduction

Ensuring a sustainable, safe, clean, and sufficient water supply is a global challenge. Advancements in science and nanotechnology have integrated nanoparticles (NPs) into numerous aspects of our lives, bringing remarkable benefits across a wide range of applications. However, the overproduction and widespread use of NPs have led to their unavoidable release into aquatic environments. This raises a critical concern: are the excess amounts of NPs in the environment negatively impacting natural ecosystems and human health. To address this concern, it is crucial to focus on the sensitive detection of NPs released into natural environments and the examination of their toxic effects.[1]

Among these NPs, titanium dioxide ($TiO_2$NPs) stands out as one of the most produced and widely used metal oxide semiconductors globally. Its low cost, versatile structure, and advanced optical properties make it highly desirable in a multitude of products and applications, including cosmetics, foods, paints, textiles, electronics, water treatment, and solar energy conversion and storage.[2,3] Although they offer advanced properties and benefits in various applications, it is an inevitable fact that their high levels of release into the aquatic environment, resulting from overproduction and widespread use, pose potential toxic risks to nature.[4–7] While $TiO_2$NPs are considered nontoxic under certain conditions, their safety depends on careful consideration of their physical and chemical properties, as well as their intended use and potential exposure levels. Importantly, these NPs are known for their photocatalytic activity, which leads to the formation of reactive oxygen species (ROS) upon exposure to light. ROS, including free radicals and peroxides, are highly reactive molecules that can cause oxidative stress in living organisms.[8–11]

For instance, in marine environments, the presence of $TiO_2$NPs and their ROS production can have profound toxic effects on aquatic life. This includes impairing the growth and biogeochemistry of marine organisms, disrupting microbial communities, and potentially altering the overall ecology and chemistry of marine systems. Therefore, understanding ROS-associated toxicities of $TiO_2$NPs and assessing their environmental risks is fundamental for developing strategies to reduce their harmful effects on natural ecosystems.

To achieve this, the priority should be the precise detection of released $TiO_2$NPs which are responsible for ROS production in the aquatic environment. While numerous laboratory analysis methods and devices have been used for the detection, collection, and quantification of $TiO_2$NPs released into the environment, significant challenges are inherent in these techniques.[12–19] For instance, NPs collected from seawater must undergo some pre-treatments such as etching, centrifugation, and filtration, and furthermore, NPs generally have high detection limits. Additionally, analysis may reveal colloids, aggregates, larger molecules, or elemental titanium, which do not provide accurate information regarding the photo-reactivity

[a] E. Tiryaki, A. Sousa-Castillo, M. A. Correa-Duarte
CINBIO, Universidade de Vigo, 36310 Vigo, Spain

[b] E. Tiryaki, A. Sousa-Castillo, M. A. Correa-Duarte
Biomedical Research Networking Center for Mental Health (CIBERSAM), Universidade de Vigo, Spain

[c] L. Rodríguez-Lorenzo, B. Espiña
Water Quality Group, INL-International Iberian Nanotechnology Laboratory, Av. Mestre José Veiga, 4715-330 Braga, Portugal

[d] R. A. Alvarez Puebla
ICREA–Institució Catalana de Recerca i Estudis Avançats, 08010 Barcelona, Spain
E-mail: ramon.alvarez@urv.cat

[e] R. A. Alvarez Puebla
Department of Physical and Inorganic Chemistry, Universitat Rovira i Virgili, 43007 Tarragona, Spain

Supporting information for this article is available on the WWW under https://doi.org/10.1002/cctc.202401002

of their nanoparticle forms. Therefore, it is still urgent to develop highly sensitive, easy-to-implement, and cost-effective methods to analyze $TiO_2$NPs and their photoactivity in aquatic systems.[19–23]

Interestingly, a colorimetric sensor has been developed to identify the presence of $TiO_2$NPs through photocatalytic dye degradation under UV light,[22] leveraging their wide band gap (3.0 eV for rutile and 3.2 eV for anatase). The interaction with UV light triggered photocatalytic reactions that produced ROS, which then degraded nearby organic dyes. Although this colorimetric method offers a way to understand the presence of these particles related to their ROS production ability within a single system, it falls short in quantifying $TiO_2$NPs concentrations. This is because the environment contains diverse $TiO_2$NPs with varying sizes and crystallinities, leading to different photocatalytic activities and dye degradation profiles. This variability makes quantification challenging, particularly in complex environments like seawater. Moreover, the ocean is home to various species and microorganisms capable of producing ROS under UV light.[23] This factor not only affects measurements but also renders the use of commercial probes for ROS quantification ineffective. Hence, there is a pressing need to develop simple and cost-effective methods not only for detecting $TiO_2$NPs in aquatic systems but also for assessing their photocatalytic activity in terms of ROS production. This would enable the establishment of an environmental risk measurement parameter.

In this framework, investigating ROS production under visible-light irradiation, rather than UV light, will enable more accurate detections by preventing UV-induced ROS production from non-targeted species. Various approaches have been utilized to enhance light absorption and improve the performance of visible-light responsive $TiO_2$-based materials for efficient solar energy utilization. These strategies include bandgap engineering through the use of plasmonic materials, heteroatom doping, and the introduction of defects, constructing heterojunctions by coupling with narrow band gap semiconductors, and modification using up conversion materials as photosensitizers.[3,25]

In this study, we introduce a novel system designed to address this urgent need: a plasmonic membrane constructed using TiNWs functionalized with AuNSts. This membrane is designed to capture and detect the presence of $TiO_2$NPs, as well as quantify their photocatalytic activity by measuring the RhB degradation in complex environments, including seawater. TiNWs have proven to be effective membranes for collecting $TiO_2$ of different sizes, facilitated by their porous structure and electrostatic interactions between the functionalized NWs and NPs. The presence of $SiO_2$-coated AuNSts significantly enhances the photocatalytic activity of $TiO_2$NPs in the visible spectrum, resulting in a significant decrease in the detection limit and reducing the reliance on UV light, thus minimizing potential interference from other species present in complex media, such as seawater. Additionally, the silica coating of the AuNSts prevents rapid electron-hole pair recombination observed in bare AuNSts, thereby preserving a linear degradation dependence on $TiO_2$NP concentration. In contrast to previous studies, the detection and evaluation of $TiO_2$NP photoactivity, specifically in terms of their ROS production ability, were conducted simultaneously and in real-time using a novel plasmon-based membrane accumulation system. This approach introduces an environmental risk parameter, enhancing our understanding of the potential ecological impact of these NPs.

## 2. Results

### 2.1. Synthesis and Characterization of Plasmonic Hybrid Membranes Filtering System

Figure 1 presents the microscopic characterization of the engineered hybrid membrane filtration setup. Initially, we synthesized one-dimensional (1D) TiNWs using the Huang method as a template material.[26] This choice was made for its superior mechanical strength, enabling the adsorption of pre-synthesized entities and providing greater flexibility in fine-tuning properties of the composite material.[27] For that, commercial $TiO_2$NPs with a diameter of 5 nm were subjected to a hydrothermal process at 240 °C for a duration of 8 hours in the presence of an alkaline solution (more details in the Materials and Methods section). This method, relying on a collaborative oriented attachment–Ostwald ripening (OA–OR) mechanism, initiates the development of an intermediate nanotube structure, which further progresses into the more thermodynamically favorable nanowire configuration. The obtained TiNWs have homogeneous elongated morphologies as can be seen in transmission electron microscopy (TEM) (Figure 1a) and field emission scanning electron microscopy (FESEM) images (Figure 1b). Average lengths of ~8 μm were characterized at diameters of 266 nm with high aspect ratios (an average of ~28.8) (Figure S1). Subsequently, to achieve a sequential adsorption of the different components, a layer-by-layer (LbL) protocol was performed by coating the TiNWs surface with positively charged polyelectrolyte of poly (allylamine hydrochloride) (PAH).[28] This synthetic approach not only ensures exceptional colloidal stability for the system but also grants a high level of precision in depositing the metal and semiconductor materials onto the support.[29] The immobilization of $TiO_2$NWs on the surface and within a membrane framework was placed using a vacuum filtration system providing advantages, particularly with regard to photocatalyst recovery and uninterrupted operation. Figure 1e shows the as-synthesized TiNWs placed onto a nylon membrane, and their distribution on the membrane was characterized by SEM analysis (Figure 1f). Finally, aqueous dispersions containing certain amounts of $TiO_2$NPs were accumulated through this membrane. The resultant TiNWs@PAH\$TiO_2$NPs nanostructures were collected for photoactivity studies (Figure 1 g).

To broaden the range of excitation wavelengths in the visible and near-infrared (NIR) regions of the electromagnetic spectrum, plasmonic nanoparticles (NPs) are exceptional photosensitizers due to their ability to efficiently harvest visible and NIR photons.[10,11] In this context, AuNSts with anisotropic morphology were preferred due to their ability to generate

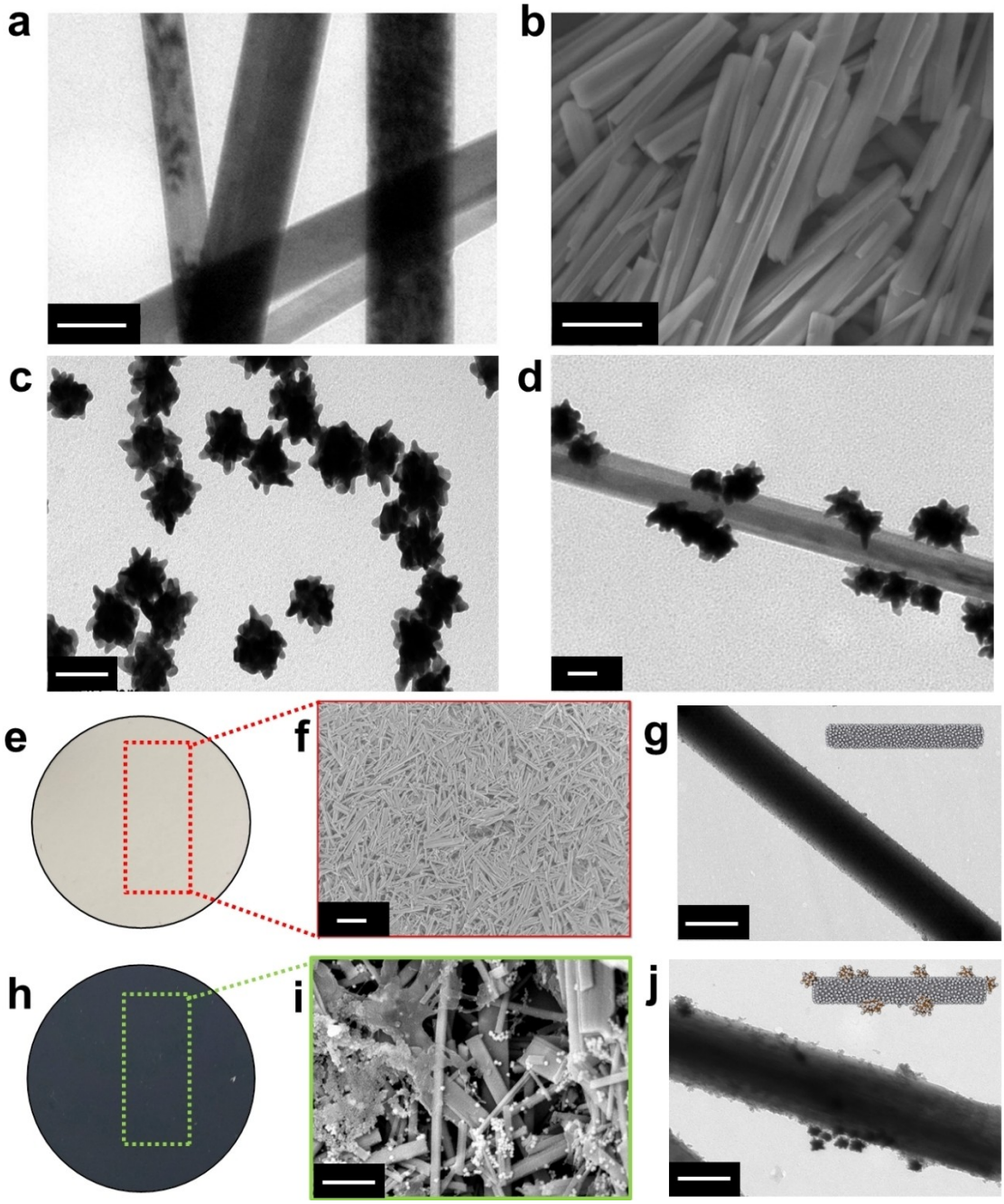


**Figure 1.** TEM and FESEM images of titanate nanowires (TiNWs) (a, b. Scale bar 200 nm and 1 μm respectively), TEM images of AuNSts and TiNWs@PAH \AuNSts (c, d. Scale bar 100 nm) TiNWs on a naylon membrane (e), SEM image from TiNWs membrane (f. Scale bar 10 μm), TEM image of TiNWs@PAH\$TiO_2$ structure obtained by filtration of $TiO_2$NPs (g. Scale bar 10 μm), TiNWs@PAH\AuNSts on a nylon membrane (h), SEM and TEM images TiNWs@PAH\AuNSts \$TiO_2$NPs after filtration system (i, j. Scale bar 1 μm and 500 nm respectively).

intense electromagnetic fields at their tips.[29] Thus, plasmonic AuNSts (depicted in Figure 1c), at different concentrations (0.08, 0.1, and 0.2 mM), were attached to positively charged TiNWs@PAH to enhance photocatalytic efficiency under visible light irradiation (as shown in Figure 1d). The synthesized plasmonic membranes were utilized to collect $TiO_2$NPs through filtration and to detect their presence based on the enhanced photocatalytic activities. The membrane composed of TiNWs@PAH \AuNSts\$TiO_2$NPs exhibited a blue color attributed to the presence of AuNSts (depicted in Figure 1h). Additionally, the SEM image in Figure 1i clearly depicts collected $TiO_2$NPs on TiNWs@PAH\AuNSts structures, while Figure 1j illustrates the TEM image of TiNWs@PAH\AuNSts\$TiO_2$NPs structures after filtration of $TiO_2$NPs.

Regarding the optical properties of the AuNSts, two distinct bands were observed, corresponding to the core (a shoulder at 550 nm) and the outer peaks (a broad band centered at 780 nm), which are typical of these nanostructures. Further-

more, the UV-visible spectra of TiNWs\AuNSts exhibited a strong absorption band at lower wavelengths, which was absent in the spectra of the free plasmonic objects in solution. This phenomenon arises from both the high absorption in the UV region and the significant contribution to scattering by the TiNWs. However, with an increase in the concentration of AuNSts, their characteristic plasmonic band became more evident (refer to Figure 2).

### 2.2. Plasmon-Assisted Photocatalysis Studies

The photocatalytic efficiency of these composites was assessed by examining the photodegradation of rhodamine B (RhB) as a model reaction, tracking the decrease in absorbance (554 nm) of this dye over time under irradiation with a solar simulator ($\lambda = 350–2400$ nm). It is noteworthy to highlight the different RhB photodegradation profiles observed for various $TiO_2$NPs sizes (5 nm, 15 nm, 25 nm), as well as for the same nanoparticles dispersed in different water media when irradiated with UV light (refer to Figure S2). This clearly demonstrates the diverse photocatalytic activity among particles dispersed in different media, hindering the identification of the specific type of $TiO_2$NPs present in a water sample. More importantly, they provide valuable insights into their photocatalytic activity in terms of ROS production, serving as a key parameter to assess the environmental risk associated with these nanomaterials.

The resulting membrane, comprising TiNW@PAH\$TiO_2$ or TiNW@PAH\AuNSts\$TiO_2$ nanocomposites, was formed after collecting $TiO_2$NPs from samples with varying $TiO_2$ concentrations and water sources. These nanocomposites were subsequently dispersed in a RhB solution ($1.0\times10^{-5}$ M) and exposed to visible light. As expected, the photocatalytic activities of $TiO_2$NPs on the titanate membranes increased in direct proportion to their concentrations, resulting in 5%, 15%, and 45% degradation of RhB in the presence of 1 ppm, 5 ppm, and 10 ppm $TiO_2$NPs, respectively (refer to Figure 3a). It is important to note that this degradation occurs as a result of the direct photoexcitation of $TiO_2$NPs, with UV photons ranging from 350–400 nm utilized from our irradiation source, which covers a broader spectrum from 350–2400 nm.

Subsequently, hybrid photocatalysts were irradiated using varying amounts of AuNSts (0.08, 0.1, and 0.2 mM), while maintaining a constant amount of semiconductor (5 ppm). However, contrary to expectations, the photocatalytic activities did not increase in direct proportion to the concentration of AuNSts (Figures 3b and S3a). Although the activity initially increased with the addition of AuNSts, reaching an optimal concentration (from 0.08 mM to 0.1 mM), further increases led to a decrease in photoactivity, attributed to an increase in electron-hole recombination. This adverse effect has been

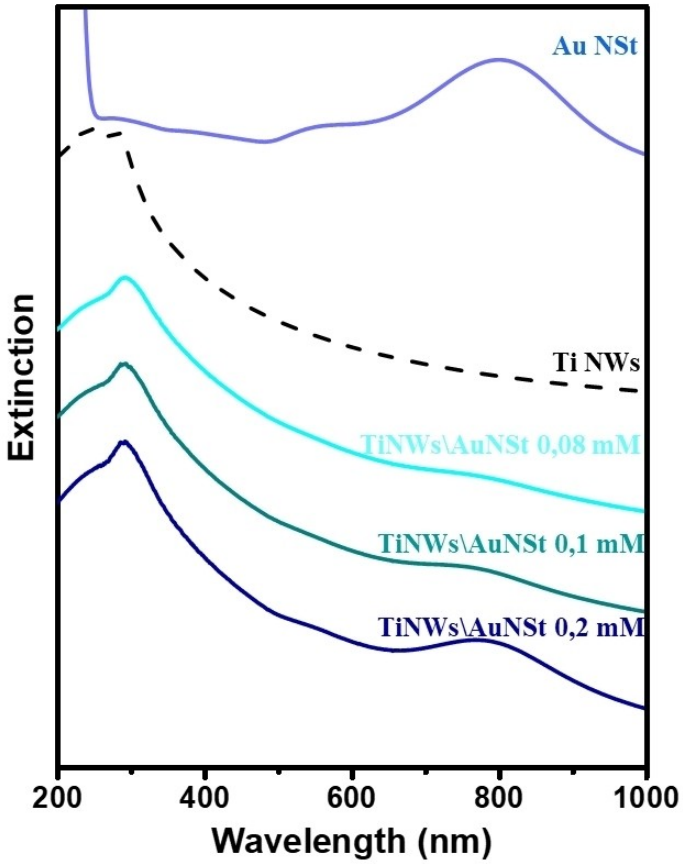


**Figure 2.** Extinction spectra of all the structures including AuNSts alone, TiNWs alone, TiNWs\AuNSts composites with different amounts of AuNSts.

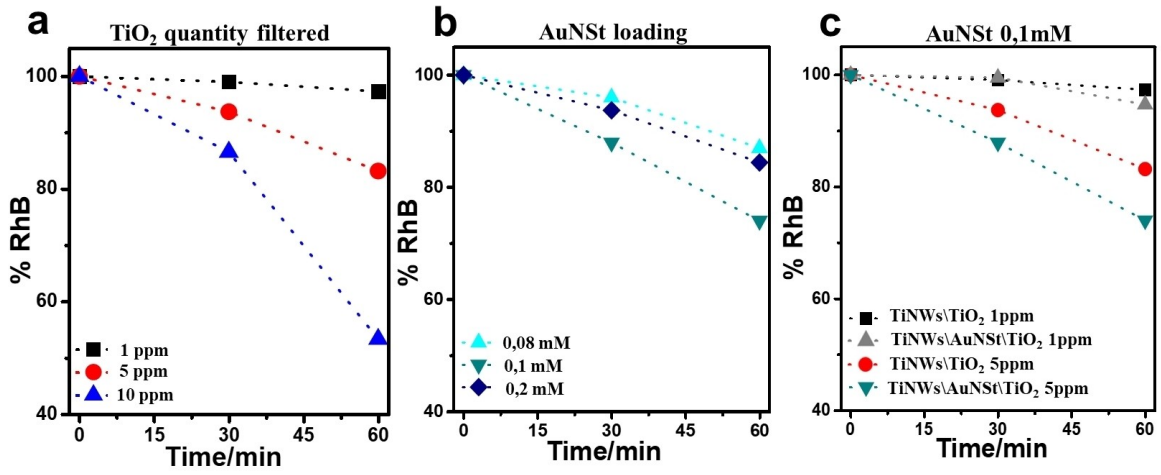


**Figure 3.** RhB photo-degradation by TiNWs\$TiO_2$ catalyst with, varying amounts of $TiO_2$NPs (a), varying concentrations of AuNSts and 5 ppm of $TiO_2$NPs (b), and varying amounts of $TiO_2$NPs and 0.01 mM of AuNSts (c).

previously elucidated as excess amounts of metals act as recombination centers which can shorten the lifetime of photo-generated hot carriers. In addition, excessive amounts of metal nanostructures can occupy the surface of the material, inhibiting interactions with light.[29,30] Consequently, the Au:Ti molar ratio should be optimized in order to obtain enhanced photocatalytic activities.[27,29] Finally, different amounts of $TiO_2$NPs were filtered through the optimized plasmonic membrane system with 0.1 mM of AuNSts, and the change in photocatalytic activity was evaluated based on the $TiO_2$NPs concentration (Figures 3c and S3b). However, while an increase in photodegradation can be observed with 5 ppm, it has been observed that at lower concentrations of $TiO_2$NPs (1 ppm), the system loses sensitivity and exhibits reduced activity. This is attributed to both the lower concentration of the semiconductor photocatalyst and a non-optimal Au:Ti molar ratio.

In previous studies, a plasmon-induced energy transfer (PET) approach has been proposed to address limitations that may arise during the hot electron injection mechanism between metal-semiconductor interfaces.[31] This approach relies on inducing photosensitization and charge separation in the semiconductor through the transmission of plasmonic energy from metals. Typically, this occurs via an insulating material positioned between the semiconductor and the metal, preventing direct contact and thus minimizing hot electron injection. To address the limitations arising from the challenge of achieving an optimum Au–Ti ratio, particularly when collecting $TiO_2$NPs from water samples with unknown $TiO_2$ concentrations, an insulating silica layer was introduced at the Au-$TiO_2$ interface. This layer serves to prevent electron-hole recombination during the hot electron injection process and enhance the photoactivity of $TiO_2$NPs, especially at low concentrations in seawater, through the plasmon-induced energy transfer (PET) mechanism. To achieve this, AuNSts were coated with silica layers of varying thicknesses, and their photocatalytic activities were evaluated. TEM images (Figure 4a) demonstrated that the AuNSts were uniformly coated with silica layers using the Stöber method. By employing different concentrations of the silica precursor, tetraethyl orthosilicate (TEOS), silica-coated AuNSts with three distinct silica thicknesses (2.6 nm, 7.4 nm, and 9.4 nm) were obtained (refer to Figure S4).

The photocatalytic studies (refer to Figure S5) conducted on TiNWs loaded with AuNSts coated with a silica layer approximately 7.4 nm of thickness demonstrated significantly enhanced activity compared to bare stars or those coated with a thinner silica layer (2.6 nm). This enhancement enabled the system to completely degrade the RhB dye and effectively lower the detection limit of $TiO_2$NPs. However, increasing the silica thickness beyond 9.4 nm resulted in a significant decrease in the activity of the plasmonic hybrid system.

Finally, the optimal AuNSts@$SiO_2$ (0.1 mM, with a 7.4 nm silica layer thickness) decorated on TiNWs hybrid system was utilized as a membrane, and $TiO_2$NPs in real seawater sample were filtered through this system (refer to Figure 4b). TEM images confirmed the homogeneous distribution of silica-coated AuNSts (refer to Figure 4b) and the collection of $TiO_2$NPs through their filtration (refer to Figure 4c). Experimentally, the silica coating onto AuNSts significantly enhanced the colloidal stability of the AuNSts, ensuring more uniform attachment to the TiNWs. The extinction spectra of AuNSts@$SiO_2$ with a 7.4 nm layer exhibited a slight blue shift at the maximum plasmon peak of the AuNSts (Figure S6). Typically, silica-coated particles display a redshift in their plasmon peaks due to changes in the refractive index of the medium. However, in our case, the presence of a sufficiently thick silica layer led to a blue shift. This phenomenon is attributed to increased scattering, which masks the plasmon band and causes the absorbance to shift to shorter wavelengths.[32]

The photocatalytic degradation of RhB dye in the presence of TiNWs\AuNSts\$TiO_2$NPs and TiNWs\AuNSts@$SiO_2$\$TiO_2$NPs catalysts is illustrated in Figure 4d. The activity of the obtained catalyst system was evaluated, considering the environment of the collected $TiO_2$NPs, Milli-Q water or seawater. Although a slight decrease in activity was observed in the case of the seawater sample, the activity remained enhanced compared to $TiO_2$NPs alone. Moreover, the obtained system retained its

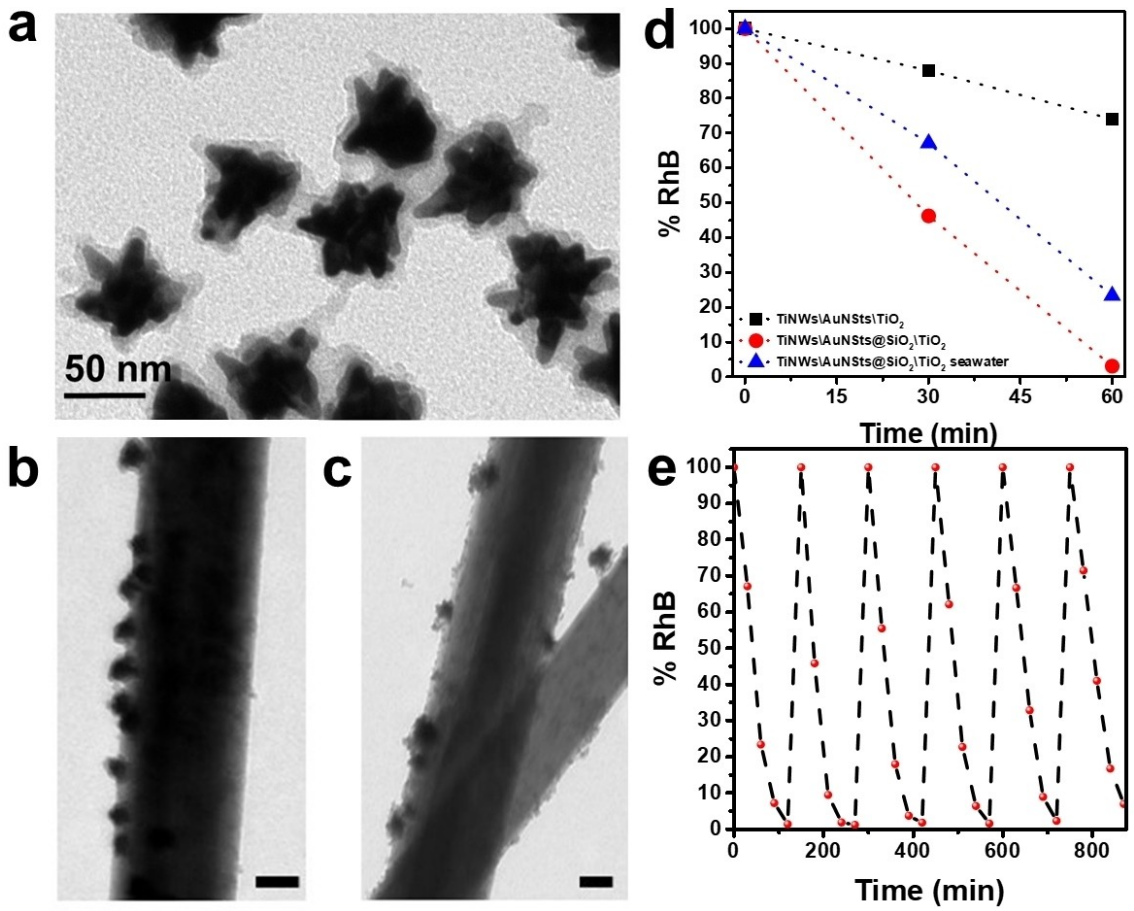


**Figure 4.** TEM images of AuNSts@$SiO_2$ (a), TiNWs\AuNSts@$SiO_2$ (b) and TiNWs\AuNSts@$SiO_2$\$TiO_2$NPs (c), RhB photo-degradation by synthesized catalysts with $TiO_2$NPs filtrated from Milli-Q water or seawater (d, scale bar 50 nm), RhB photodegradation ability of the catalyst after 6 repeated degradation studies (b and c scale bar 50 nm).

stability even after six successive photocatalysis studies (refer to Figure 4e). These results confirm that the designed plasmonic membrane is highly effective for collecting, detecting, and evaluating the catalytic activity of $TiO_2$NPs from seawater, even at low concentrations.

## 3. Conclusions

Herein, we presented hybrid filter system based on titanate nanowires to monitor in real time $TiO_2$ NPs from seawater and determine their dosages with high sensitivity through their photocatalytic activities. During the photocatalytic evaluation of $TiO_2$ NPs, irradiation by a solar light source with cut-off UV light, the selective detection of free radicals originating from $TiO_2$ NPs were achieved. Thus, a new approach has been proposed for the detection of photoactive NPs forms accumulated in high amounts in seawater, which is one of the major environmental problems nowadays. With the plasmon-enhanced photocatalytic reactions of $TiO_2$ NPs, which are easily collected in the developed filter system, selective detection is achieved without the need for expensive analysis methods or pre-processes.

To enhance the detection limit of $TiO_2$ NPs, Ti NWs were decorated with plasmonic Au NSts. The TiNWs\AuNSts hybrid filter system we have developed offers several advantages; (i) $TiO_2$ NPs were collected and concentrated effectively by filtration through positively charged TiNWs\AuNSts which have high surface area and anisotropic morphology. Moreover, Ti NWs as templates with high aspect ratios provided a homogeneous distribution of plasmonic Au NSts, which prevented agglomerations that can reduce their photocatalytic efficiency. (ii) Thanks to the LbL assembly, close physical interfaces were formed between plasmonic Au NSts and $TiO_2$ NPs. Thus, by providing an effective plasmon-semiconductor interaction, possible photocatalysis mechanisms such as localized surface plasmon resonance (LSPR)-mediated hot electron injection was enabled. (iii) Plasmonic Au NSts integrated onto the titanate membrane assisted the photocatalytic activities of $TiO_2$ NPs collected on the filter under solar light irradiation. (iv) The coating of plasmonic Au NSts with an insulating silica layer minimized electron-hole recombination, enabling the photocatalytic activities of $TiO_2$ NPs to be carried out with high efficiency under solar light, thus identifying $TiO_2$ NPs with detectable activity even in very low detection limits (1 ppm).

## Experimental Section

### Chemicals

Tetrachloroauric acid ($HAuCl_4 \cdot 3H_2O$), tetraethyl orthosilicate (TEOS), sodium hydroxide (NaOH), poly (allylamine hydrochloride) (PAH), sodium chloride (NaCl), trisodium citrate dihydrate ($Na_3C_6H_5O_7$), polyvinylpyrrolidone (PVP, average mol weight ~10,000), dimetilformamid (DMF), ammonium hydroxide ($NH_4OH$, 28%) and ethanol were purchased from Sigma-Aldrich (St. Louis, MO, USA). Titanium dioxide nanopowders (anatase, 5 and 15 nm size, 99%) were purchased from Nanostructured & Amorphous Materials, Inc. (Katy, TX, USA). Titanium (IV) oxide nanopowder (Aeroxide P25, 718467) was purchased from Sigma Aldrich. Milli-Q water with a resistivity higher than 18.2 MΩcm was used for all the preparations.

### Synthesis of Titanate Nanowires (TiNWs) and PAH Coating

TiNWs were synthesized via the hydrothermal method as previously reported.[27] 0.2 g of $TiO_2$NPs (5 nm, anatase) were added to 20 mL of 8 M NaOH aqueous solution and the solution was sonicated for a while. The prepared solution was maintained in an oven at 240 °C for 8 h. The synthesized TiNWs were washed (6000 rpm, 20 min) several times until the pH became neutral. The obtained TiNWs (5 mg) were dispersed in 50 mL of positively charged PAH solution (1 mg/mL polymer in 0.5 M of NaCl aqueous solution) and stirred for 30 min. The excess of PAH was removed by centrifugation for several times.

### Synthesis of Gold Nanostars (AuNSts) and Silica Coating

PVP-stabilized AuNSts were synthesized via the seed-mediated growth mechanism as previously described.[33] Firstly, 15 nm spherical gold seeds were synthesized by Turkevich method with some modifications.[34] Secondly, as-synthesized gold seeds ([Au] = 1 mM, 550 μL) were added into 25 mL of PVP/DMF (with 5 g of PVP) solution and AuNSts were obtained by adding $HAuCl_4$ (0.12 M, 70 μL) into the solution. The solution was mixed for 2 h and the colour of the solution was turned to dark blue in time. The synthesized AuNSts were centrifuged and washed with EtOH. The AuNSts were subsequently coated with a silica layer. For this purpose, AuNSts ([Au] = 0.75 mM) were dispersed in 10 ml of EtOH/$H_2O$ solution. 0.126 mL of $NH_4OH$ and 20 mM of 5% TEOS/EtOH solution were added and reaction was allowed to mix for 3 h. After 3 h, the silica-coated AuNSts were washed with EtOH (4500 rpm, 30 min) several times and finally redispersed in Milli-Q water.[35]

### Deposition of AuNSts onto TiNWs

The positively charged Ti NWs particles (5 mg in 25 mL $H_2O$) were added into silica-coated and un-coated AuNSts solution (0.1 mM in 25 mL $H_2O$) and mixed for overnight to supply electrostatic interaction between TiNWs and AuNSts. After mixing, the obtained hybrid particles were centrifuged and washed 2 times with $H_2O$. To provide electrostatic interactions between obtained hybrid particles and $TiO_2$NPs during filtration, hybrid particles were modified by positively charged polymer, PAH. For this purpose, PAH (1 mg/mL) was dissolved in NaCl aqueous solution (6 mM, 50 mL) and poured into the hybrid particles solution. After 30 min mixed, the PAH-coated hybrid particles were centrifuged and washed with Milli-Q water.

### Filtration of Water/Seawater Containing $TiO_2$NPs Through As-Synthesized Hybrid Particles

$TiO_2$NPs through as-synthesized hybrid particles: Briefly, 5 mg of hybrid particles were deposited onto a nylon membrane (0.20 μm pore size). After all particles were homogeneously deposited onto the membrane, water/seawater containing different amounts of $TiO_2$NPs were vacuum filtered through the deposited hybrid particles. The $TiO_2$ captured hybrid particles were separated from the membrane and added into the model organic dye Rhodamine B (RhB) solution to investigate the captured $TiO_2$NPs amount.

### Photocatalytic Assessment of Captured $TiO_2$NPs Amount

5 mg of hybrid particles with captured $TiO_2$ (5 nm) were dispersed in 20 mL of aqueous RhB solution ($10^{-5}$ M) and stirred for 1 h in the dark to provide adsorption–desorption equilibrium between the particles and RhB. This solution was injected into the AuNSt\$TiO_2$ hybrid filter with a syringe at a rate of 2 mL/h and retained on the filter. Afterwards, the solution was irradiated by solar light using a 300 W Xe lamp in a LOT-Quantum Design solar simulator (350–2400 nm) at a controlled temperature (25 °C) by circulating water through the reactor. Subsequently, aliquots of 1.5 mL were taken within 30 min intervals under irradiation with the solar simulator, allowing the quantification of the photocatalytic process by monitoring the decreasing adsorption of the RhB dye in the solution (Figure S7).

### Characterization

Transmission electron microscope (TEM) images were obtained using a JEOL JEM 1010 instrument operating at an acceleration voltage of 100 kV and equipped with a CCD camera (Tokyo, Japan). TEM samples were prepared by dropping 10 μL of NPs dispersion onto a 400 mesh Cu grid covered with carbon film and drying it at room temperature. Layer-by-layer self-assembly was confirmed by ζ-potential measurements using a Malvern Zetasizer Nano series. Field emission scanning electron microscope (FESEM) analysis were performed using a JEOL JSM-6700F microscope. Envision Multimode Plate Reader was used to measure the absorbance values of RhB dye. UV-vis-NIR spectra were obtained with a Hewlett-Packard HP 8453 spectrophotometer (CA, USA).

## *Acknowledgements*

Authors acknowledge financial support from NANOCULTURE Interreg Atlantic Area project (EAPA 590/2018), the Spanish Ministerio de Ciencia e Innovación under projects (TED2021-132101B–I00/AEI/10.13039/501100011033; PID2020-113704RB–I00/AEI/10.13039/501100011033; PDC2021-121787-I00/AEI/10.13039/501100011033; PID2020-120306RB–I00/AEI/10.13039/501100011033), Xunta de Galicia/FEDER (IN607 A 2018/5 and Centro Singular de Investigación de Galicia, Acc. 2019–2022, ED431G 2019–06). Authors acknowledge the use of scientific and technical services from Centro de Apoio Científico e Tecnolóxico á Investigación (CACTI-Universidade de Vigo) and the support from M. Spuch, L. Guillade to characterize the systems. A.S.C. acknowledges Xunta de Galicia, Spain, for her postdoctoral fellowship and Deputation de Pontevedra for her financial support (INPO23-24). L.R.-L. acknowledges funding to

FCT (Fundação para a Ciência e Technologia) for the Scientific Employment Stimulus Program (2020.04021.CEECIND).

## Conflict of Interests

The authors declare no conflict of interest.

## Data Availability Statement

The data that support the findings of this study are available from the corresponding author upon reasonable request.

**Keywords:** Titanium dioxide nanoparticles · Gold nanoparticles · Membranes · Sensor · Photocatalysis

[1] X. Huang, M. Auffan, M. J. Eckelman, M. Elimelech, J–H. Kim, J. Rose, K. Zuo, Q. Li, P. J. J. Alvarez, *Nat. Rev. Earth Environ.* **2024**. https://doi.org/10.1038/s43017-024-00567-5.
[2] H. M. R. Abdel-Latif, M. A. O. Dawood, S. Menanteau-Ledouble, M. El-Matbouli, *Ecotoxicol. Environ. Saf.* **2020**, *200*, 110776.
[3] L. Jiang, S. Zhou, J. Yang, H. Wang, H. Yu, H. Chen, Y. Zhao, X. Yuan, W. Chu, H. Li, *Adv. Funct. Mater.* **2022**, *32*, 2108977.
[4] S. A. Diamond, A. J. Kennedy, N. L. Melby, R. D. Moser, A. R. Poda, C. A. Weiss, J. A. Brame, *NanoImpact* **2017**, *8*, 11–19.
[5] J. M. Farner, R. S. Cheong, E. Mahé, H. Anand, N. Tufenkji, *Environ. Sci. Nano* **2019**, *6*, 2532–2543.
[6] J. Hou, L. Wang, C. Wang, S. Zhang, H. Liu, S. Li, X. Wang, *J. Environ. Sci.* **2019**, *75*, 40–53.
[7] S. N. A. Shah, Z. Shah, M. Hussain, M. Khan, *Bioinorg. Chem. Appl.* **2017**. https://doi.org/10.1155/2017/4101735.
[8] E. Fonseca, M. Vázquez, L. Rodriguez-Lorenzo, N. Mallo, I. Pinheiro, M. L. Sousa, S. Cabaleiro, M. Quarato, M. Spuch-Calvar, M. A. Correa-Duarte, J. J. López-Mayán, M. Mackey, M. Moreda, V. Vasconcelos, B. Espiña, A. Campos, M. J. Araújo, *J. Hazard. Mater.* **2023**, *458*, 131915.
[9] M. M. Rashid, P. F. Tavčer, B. Tomšič, *Nanomaterials (Basel)* **2021**, *11*, 9.
[10] A. Sousa-Castillo, J. R. Couceiro, M. Tomás-Gamasa, A. Mariño-López, F. López, W. Baaziz, O. Ersen, M. Comesaña-Hermo, J. L. Mascareñas, M. A. Correa-Duarte, *Nano Lett.* **2020**, *20*(10), 7068–7076.
[11] Y. Negrín-Montecelo, C. Brissaud, J.-Y. Piquemal, A. O. Govorov, M. A. Correa-Duarte, L. V. Besteiro, M. Comesaña-Hermo, *Nanoscale* **2022**, *14*, 11612–11618.
[12] L. Fu, M. Hamzeh, S. Dodard, Y. H. Zhao, G. I. Sunahara, *Environ. Toxicol. Pharmacol.* **2015**, *39*(3), 1074–1080.
[13] F. Xu, *Chemosphere* **2018**, *212*, 662–677.
[14] A. Philippe, J. Košík, A. Welle, J. M. Guigner, O. Clemens, G. E. Schaumann, *Environ. Sci. Nano* **2018**, *5*, 191–202.
[15] F. Dutschke, J. Irrgeher, D. Pröfrock, *Anal. Methods* **2017**, *9*, 3626–3635.
[16] M. Sysoltseva, R. Winterhalter, A. S. Wochnik, C. Scheu, H. Fromme, *Int. J. Cosmet. Sci.* **2017**, *39*(3), 292–300.
[17] Y. Deng, E. J. Petersen, K. E. Challis, S. A. Rabb, R. D. Holbrook, J. F. Ranville, B. C. Nelson, B. Xing, *Environ. Sci. Technol.* **2017**, *51*(18), 10615–10623.
[18] S. P. Bitragunta, S. G. Palani, A. Gopala, S. K. Sarkar, V. R. Kandukuri, *Bull. Environ. Contam. Toxicol.* **2017**, *98*, 595–600.
[19] K. Badalova, P. Herbello-Hermelo, P. Bermejo-Barrera, A. Moreda-Piñeiro, *J. Trace Elem. Med. Biol.* **2019**, *54*, 55–61.
[20] Z. X. Luo, Z. H. Wang, B. Xu, I. L. Sarakiotis, G. Du Laing, C. Z. Yan, *J. Zhejiang Univ. Sci. A* **2014**, *15*(8), 593–605.
[21] A. Gondikas, F. Von Der Kammer, R. Kaegi, O. Borovinskaya, E. Neubauer, J. Navratilova, A. Praetorius, G. Cornelis, T. Hofmann, *Environ. Sci. Nano* **2018**, *5*, 313–326.
[22] A. Praetorius, A. Gundlach-Graham, E. Goldberg, W. Fabienke, J. Navratilova, A. Gondikas, R. Kaegi, D. Günther, T. Hofmann, F. Von Der Kammer, *Environ. Sci. Nano* **2017**, *4*, 307–314.
[23] G. Bulbul, H. Eskandarloo, A. Abbaspourrad, *Anal. Methods* **2018**, *10*, 275–280.
[24] J. J. Morris, A. L. Rose, Z. Lu, *Redox Biol.* **2022**, *52*, 102285.
[25] S. Zhou, L. Jiang, H. Wang, J. Yang, X. Yuan, H. Wang, J. Liang, X. Li, H. Li, Y. Bu, *Adv. Funct. Mater.* **2023**, 2307702. https://doi.org/10.1002/adfm.202307702.
[26] J. Huang, Y. Cao, Q. Huang, H. He, Y. Liu, W. Guo, M. Hong, *Cryst. Growth Des.* **2009**, *9*(8), 3632–3637.
[27] Y. Negrín-Montecelo, M. Testa-Anta, L. Marín-Caba, M. Pérez-Lorenzo, V. Salgueiriño, M. A. Correa-Duarte, M. Comesaña-Hermo, *Nanomaterials (Basel)* **2019**, *9*(7), 990.
[28] F. Caruso, R. A. Caruso, H. Möhwald, *Science* **1998**, *282*(5391), 1111–1114.
[29] A. Sousa-Castillo, M. Comesaña-Hermo, B. Rodríguez-González, M. Pérez-Lorenzo, Z. Wang, X. T. Kong, A. O. Govorov, M. A. Correa-Duarte, *J. Phys. Chem. C* **2016**, *120*(21), 11690–11699.
[30] A. Bumajdad, M. Madkour, *Phys. Chem. Chem. Phys.* **2014**, *16*(16), 7146–7158.
[31] Y. Negrín-Montecelo, X. T. Kong, L. V. Besteiro, E. Carbó-Argibay, Z. M. Wang, M. Pérez-Lorenzo, A. O. Govorov, M. Comesaña-Hermo, M. A. Correa-Duarte, *Appl. Mater. Interfaces* **2022**, *14*(31), 35734–35744.
[32] L. M. Liz-Marzán, M. Giersig, P. Mulvaney, *Langmuir* **1996**, *12*(18), 4329–4335.
[33] P. Senthil Kumar, I. Pastoriza-Santos, B. Rodríguez-González, J. F. García De Abajo, L. M Liz-Marzán, *Nanotechnology* **2008**, *19*(1), 015606.
[34] J. Turkevich, P. C. Stevenson, J. Hillier, *Discuss. Faraday Soc.* **1951**, *11*, 55–75.
[35] W. Stober, A. Fink, D. Ernst Bohn, *J. Colloid Interface Sci.* **1968**, *26*, 62–69.

Manuscript received: July 9, 2024
Revised manuscript received: August 8, 2024
Accepted manuscript online: August 9, 2024
Version of record online: October 21, 2024